

# STUDY ON THE P FACTOR OF TILLAGE PRACTICES IN THE TYPICAL BLACK SOIL AREAS OF NORTHEAST CHINA UNDER EXTREME RAINFALL CONDITIONS

JIAO, J.<sup>1</sup> – QIN, W.<sup>1,2\*</sup> – LI, K.<sup>3</sup> – YIN, Z.<sup>1,2</sup>

<sup>1</sup>State Key Laboratory of Simulation and Regulation of Water Cycle in River Basin, China  
Institute of Water Resources and Hydropower Research, Beijing 100048, PR China  
(phone: +86-10-6878-6380)

<sup>2</sup>Research Center on Soil and Water Conservation of the Ministry of Water Resources, Beijing  
100048, PR China  
(phone: +86-10-6878-6956)

<sup>3</sup>College of Mining Engineering, Liaoning Technical University, Fuxin 123000, PR China  
(phone: +86-418-511-0025)

\*Corresponding author

e-mail: qinwei@iwhr.com; phone: +86-10-6878-6380

(Received 2<sup>nd</sup> May 2021; accepted 30<sup>th</sup> Aug 2021)

**Abstract.** The support practice factor (P) is an essential component of the common Universal Soil Loss Equation (USLE) model. Although concerns about soil loss in the typical black soil areas of Northeast China are increasing, little research exists on the P factor of extreme rainfall in soil loss. Therefore, we conducted an orthogonal simulation experiment of artificial rainfall employing different rainfall intensities, slopes, and tillage practices. The aim of the design was to establish the values and calculation methods for the P factor of different tillage practices under various slope and rainfall intensity conditions. Our results showed that for No tillage (NT) and longitudinal wide ridge (LWR), a significant logarithmic decreasing relationship was found between the P factor and the product of rainfall erosivity (R) and slope factor (S). When  $RS$  was  $< 9.18$  MJ·mm/(hm<sup>2</sup>·h), contour ridge tillage was the optimal practice to decrease soil loss. The P factor of contour narrow ridge (CNR) was higher than those of other tillage practices after contour ridge failure occurred. When maximum rainfall intensity was  $> 75$  mm/h, NT was superior in reducing soil loss. The results could provide a basis for predicting soil loss under extreme rainfall conditions.

**Keywords:** USLE, simulation experiment, rainfall erosivity, slope factor, hydraulic characteristic, ridge system

**Abbreviations:**  $A$ : soil loss modulus,  $A_F$ : soil loss modulus for contour ridge failure, CNR: contour narrow ridge, CWR: contour wide ridge,  $D$ : runoff depth,  $Fr$ : Froude number, LNR: longitudinal narrow ridge, LWR: longitudinal wide ridge,  $n$ : roughness, NT: no tillage,  $Q_r$ : runoff volume measured by the flowmeter at the outlet of the soil tank,  $R$ : rainfall erosivity,  $S$ : slope factors,  $V_F$ : volume for soil loss for contour ridge failure,  $W_F$ : width for soil loss for contour ridge failure

## Introduction

Soil loss is a crucial factor in the loss and degradation of land resources that humans depend on for survival. To provide suggestions on reducing the loss of soil, a tool able to diagnose the “problem” of soil loss is required to provide the scientific basis for preventing and controlling the occurrence and aggravation of such a loss. This tool is the soil loss model (Lane et al., 1992; Kinnell, 2010; Di Stefano et al., 2019). In regard to soil modelling mean, soil loss models can be categorised as either empirical or mechanistic (Aksoy and Kavvas, 2005; Batista et al., 2019). Empirical models are a series of

mathematical equations based on the statistical analysis of a large amount of experimental observation data (Foster et al., 2001; Khosravi et al., 2012). Mechanistic models are primarily based on physical causes and quantitatively describe and depict the soil loss process by simulating various effects (Nearing et al., 1989; Licznar and Nearing, 2003; Nouwakpo et al., 2018). These effects include rainfall infiltration, runoff formation, raindrop splashing, and runoff scouring on a series of main processes, such as soil separation, sediment transport and deposition, plant growth, and stubble decomposition. Empirical soil loss models are applied widely because of their low input requirements for parameters and variables (Kinnell and Risse, 1998; Ibearugbulem et al., 2018). However, mechanistic models are still in the research stage in most countries and regions and have not been applied widely because of the difficulty to obtain model parameters, operate the models (Shoemaker et al., 2005; Lobo and Bonilla, 2019), and the cost is high.

Among the empirical models, the Universal Soil Loss Equation (USLE) has a long application history and wide application scope (Wischmeier and Smith, 1958; Ahamed et al., 2000; Tyner et al., 2011). Its first official version was launched through Agricultural Manual No. 282 in 1965 (Wischmeier and Smith, 1965) and the second version was launched through Agricultural Manual No. 537 in 1978 (Wischmeier and Smith, 1978). In 1997, the Revised Universal Soil Loss Equation (RUSLE) was released officially (Renard et al., 1997). The USLE includes the main factors that affect soil loss on a sloping surface and uses a wide range of data; hence, it has been applied widely in rainfall soil loss prediction in many countries to conduct soil loss investigations (Yu et al., 1999; Van der Kinff et al., 2000; Mausbach and Dedrick, 2004; Brazier, 2016). In 1975, the Soil Health Institute in the United States developed the MUSLE (Modified Universal Soil Loss Equation) model based on USLE, which can simulate soil loss at the watershed scale with a single rainfall event as the simulation step (Williams, 1975). Since then, MUSLE has been adopted by the crop productivity model (Williams et al., 1983), watershed non-point source pollution model (Gassman et al., 2007), and others (Shoemaker and Dai, 2005), and has played an important role in the simulation of the surface ecological process. The factors that affect the soil loss used in this model, such as soil erodibility, slope length, coverage, management measures, and soil conservation measures, have the same meanings as those in the USLE.

According to the definition of the Universal Soil Loss Equation, the P factor for soil conservation practices refers to the soil loss ratio with the implementation of conservation measures when directly tilling up and down along a sloping farmland. Such soil conservation measures can be divided into two categories, namely engineering measures and tillage practices (Liu et al., 2002; Xin et al., 2019). Engineering measures reduce soil loss by changing a certain scope of the micro-topography (e.g., terraces) to retain surface runoff and increase rainfall infiltration. Tillage practices involve improving the anti-soil-loss performance of the soil, preserving water and soil and preventing soil loss through farming, specifically by using ploughs, hoes, harrows, and other farming tools or machinery to increase surface coverage, increase soil infiltration, and the like. The difference between tillage practices and engineering measures is that the former does not change the micro-topography and is implemented only on agricultural land. The establishment of a soil loss model is primarily based on a large quantity of observations and experimental data. Long-term, high-quality experimental and monitoring data comprise the basis for establishing this model and are an important and reliable means to obtain the P factor (Chen et al., 2017). When calculating the P factor, with regard to the kind of underlying surface and tilling methods that should be

considered as the objects for reference and contrast, USLE and RUSLE stipulate up-and-down slope culture (Wischmeier and Smith, 1978; Renard et al., 1997). However, under the same longitudinal tillage method, the soil loss amount could differ substantially because of different tillage systems with different ridge spaces, widths and heights (Xu et al., 2019). Therefore, the objects for reference and contrast should be further concretised.

Soil loss has become increasingly concerning in the typical black soil areas of Northeast China (Lal et al., 2001; Liu et al., 2008), which comprise approximately 17.27 million hm<sup>2</sup> of cropland, accounting for 14% of total croplands in China. Longitudinal ridge tillage has been a common practice for a long time in this area; typical sampling survey in Heilongjiang Province showed that 3/4 of the farmland has adopted longitudinal or quasi-longitudinal ridge tillage practices (Zhao et al., 2012). In recent years, with the promotion of black soil land protection, soil loss prevention measures have been popularised and implemented gradually. Black soil areas are an important commodity grain base, and are the main producers of crops such as sugar beet, flax, and sunflower (Cui et al., 2007; Wang et al., 2015). To ensure farmland quantity and grain output, implementing vegetation measures such as returning farmland into forest or grassland is not suitable. At present, in the distribution zones of black soil and chernozem in these typical black soil areas, nearly half of the black soil layers in the profiles have a thickness of < 40 cm, whereas in the chernozem distribution areas, the thickness of black soil layers in more than half of the profiles is < 20 cm (Wang et al., 2009). If soil conservation engineering measures were implemented, the excavation depth in the thin soil layer would exceed the tillage layer, leading to the destruction of surface soil resources. Therefore, soil conservation tillage practices currently comprise the main method to prevent and control soil loss in these areas.

Recommendations to improve soil and water conservation include adjusting longitudinal ridge tillage to contour ridge tillage or no tillage (NT). Research has been conducted on the effects of such tillage practices on soil and water loss and sediment reduction, and the conservation tillage practices in these areas could increase gradually in the future (Xu et al., 2018; Zhang et al., 2012). However, few studies have been conducted on the P factor values of different tillage practices in this area and, particularly, no studies could be located on calculating the P value under extreme rainfall conditions.

A high-intensity rainstorm of short duration on a slope under the contour ridge tillage system usually causes concentrated stream soil loss and intensified gully-cutting soil loss. Usually, these affects can be ascribed to the infiltration-excess runoff in the furrows gradually gathering and then breaking out from the ridges in fragile or low-lying places of the contour ridges (Meng et al., 2009). In recent years, climate change and its significant global effects on water resources, environment, ecology, and the like, have become pressing environmental problems. The fifth assessment report of the United Nations Intergovernmental Panel on Climate Change (IPCC) showed that global warming has changed the global water cycle process (Ohmura and Wild, 2002), resulting in changes in the temporal and spatial distribution of precipitation and the frequent occurrence of extreme rainfall events (Stocker et al., 2013). Research has indicated an increase in the frequency and intensity of extreme rainfall worldwide in recent decades, and this trend could continue (Singh and Kumar, 1997; Arnell, 1999; Bartholy and Pongrácz., 2007). The influence of extreme rainfall events on the effects of conservation tillage practices on soil and water requires further investigation.

In this study, we employed an indoor artificial rainfall simulation experiment to determine the reference objects for calculating the P factor; furthermore, we propose calculation methods for the P factor value under different slope and rain intensities with the purpose of predicting soil loss.

## Materials and methods

### *Materials*

The soil used in the experiment was obtained from a long, gentle sloping farmland from the Soil and Water Conservation Experimental Station in Keshan County, Heilongjiang Province, where longitudinal ridge tillage is adopted in the field (*Fig. A1* in the *Appendix*). The slope of the plot is primarily between 3° and 5°, and the soil type is black soil. The geographical coordinates of the soil collection site are 48°03'17"N and 125°49'23"E. The location has a temperate continental monsoon climate, with an annual average temperature of 3.0 °C, and the annual average precipitation concentrated from June to September is 514.9 mm. The land plot is located at the southern foot of the Lesser Khingan Mountains in the transition zone next to the Songnen Plain. Soybean is the main crop, and mechanisation is adopted mainly in field operations.

The test soil derives from typical cultivated black soil within 40 cm from the surface of the sloping farmland. Soil particles comprise clay (<2 µm), silt (2-50 µm), and sand (50-2000 µm), accounting for 23.7%, 72.5%, and 3.8% of the soil particle composition, respectively. The soil organic matter content is 29.67 g/kg, and the pH value is 6.81.

Our artificial rainfall simulation experiment was conducted in the soil conservation hall of the Yanqing Experimental Base of the China Institute of Water Resources and Hydropower Research. The rainfall equipment comprised a side-spray artificial rainfall device, which uses computer software to control rainfall intensity in the range of 10 to 200 mm/h. The rainfall height was 13.8 m, and rainfall uniformity was more than 85%.

The dimensions of the test soil tank (fixed hydraulic lifting and descending steel tank) were 8 m × 3 m × 1 m (length × width × height) (*Fig. 1*). Tipping-bucket flowmeters were used at the runoff collector of the tank to perform measurements in the runoff yield process at a resolution of 3 L. Tipping-bucket self-recording rain gauges were used to measure the simulated rainfall at a resolution of 0.2 mm.

### *Design of the artificial rainfall simulation experiment*

We adopted an orthogonal design for the artificial rainfall simulation experiment. The primary factors we considered were rain intensity, surface slope, and tillage practices. Forty experimental sessions (4 × 2 × 5) were conducted, with two replicates for each session.

The rain intensity design of our artificial rainfall experiment was based on the intensities of the rainstorms in different recurrence periods in the soil source area. The rainfall intensities were analysed and determined, considering the reports on erosive rainfall intensities in the typical black soil areas in Northeast China. The 1 h rainstorm intensities in the 20%, 10%, 5%, 2%, and 1% recurrence periods of Keshan, where the test soil is located, are 35.7, 43.6, 49.3, 60.5, and 68.2 mm/h (Ye et al., 2014), respectively. According to Lu et al. (2016), in the heavy rainfall soil loss events with above-moderate soil loss intensities, the instantaneous rainfall intensities range from 42.6 to 103.2 mm/h. On this basis, we designed four typical rainfall intensities for this study, namely 30, 50, 75, and 100 mm/h, with the simulated rainfall events all lasting 1 h.

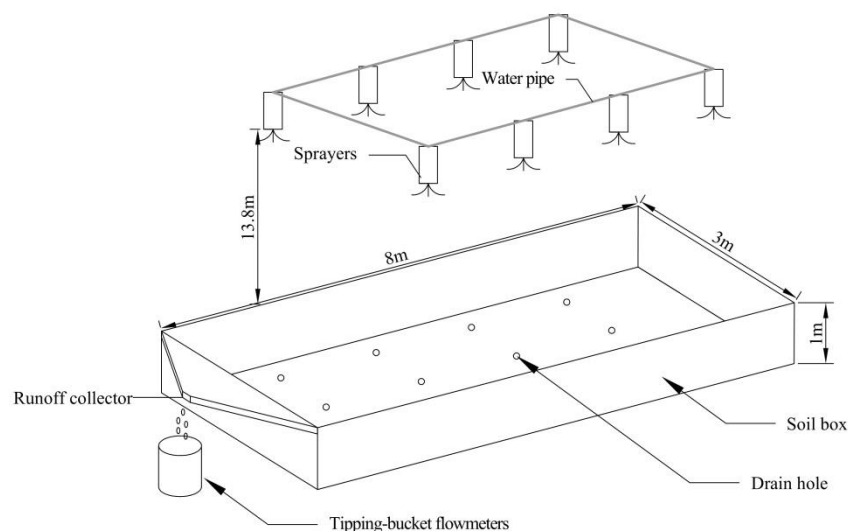


**Figure 1.** Schematic diagram of test soil tank and artificial rainfall system

Typically, black soil areas in Northeast China have gentle and long slopes. The slope of the ground of the soil collection site was mainly between  $2^{\circ}$  and  $6^{\circ}$ , and the slope length mainly between 100 and 1000 m. Therefore, two common angles of slope were designed for the experiment, with angles of  $3^{\circ}$  and  $5^{\circ}$ .

Tillage practices adopted in the sloping farmland in the source area include mainly longitudinal ridging, contour ridging, and no tillage (Chen et al., 2008; Shen et al., 2020). For ridged sloping farmland, there were two types of ridges, namely wide and narrow ridges (Xu et al., 2018). For wide ridges, the distance was 100–120 cm, width was 65–75 cm, furrow width was 35–45 cm, and height was 7–12 cm. For narrow ridges, the distance was 55–70 cm, width was 30–35 cm, furrow width was 25–35 cm, and height was 12–20 cm. Therefore, we adopted five tillage practices, namely no tillage (NT), longitudinal wide ridge (LWR), longitudinal narrow ridge (LNR), contour wide ridge (CWR), and contour narrow ridge (CNR) (Fig. 2). For wide ridges, the distance was 110 cm, ridge width was 70 cm, furrow width was 40 cm, and average furrow depth was 10 cm. For narrow ridges, the distance was 60 cm, ridge width was 30 cm, furrow width was 30 cm, and average furrow depth was 15 cm (Table 1).

**Table 1.** Comparison between actual plot conditions and experimental simulation conditions

Primary factor	Actual conditions	Simulation conditions
Rain intensity (mm/h)	1 h rainstorm intensity in 20% recurrence period is 35.7 mm/h; range of heavy rainfall intensity is between 42.6 and 103.2 mm/h	30, 50, 75, and 100
Slope ( $^{\circ}$ )	2–6	3 and 5
Slope length (m)	100–1000 m	8
Ridge furrow width (cm)	Wide ridge 35–45, narrow ridge 25–35	Wide ridge 40, narrow ridge 30
Ridge width (cm)	Wide ridge 65–75, narrow ridge 30–35	Wide ridge 70, narrow ridge 30
Ridge height (cm)	Wide ridge 7–12, narrow ridge 12–20	Wide ridge 10, narrow ridge 15

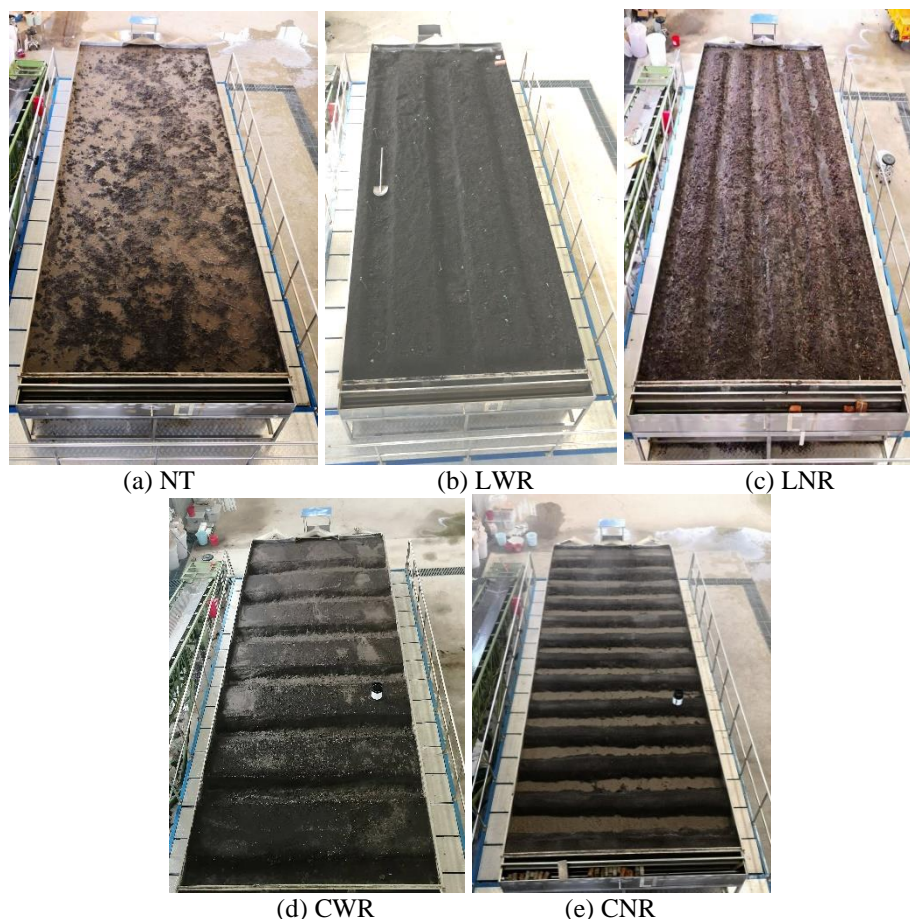


**Figure 2.** Photos of tillage practices adopted in the indoor simulation experiment

### ***Steps in the artificial rainfall simulation experiment***

(1) Before loading the soil, evenly spaced drainage holes were drilled at the bottom of the test soil tank; these drainage holes were first filled with gauze, and then with fine sand up to 20 cm in thickness to form a permeable layer and ensure adequate water permeability. The test soil tanks were filled according to the soil bulk densities of the plough pan, tilth, and ridge layers measured in the field. Above the sand layer, the plough pan layer was filled to a thickness of 30 cm with a soil bulk density of  $1.35 \text{ g/cm}^3$ , then the tilth layer was filled to a thickness of 30 cm with a soil bulk density of  $1.20 \text{ g/cm}^3$ . The layered filling method was adopted; with one layer every 5 cm. Additionally, when filling the soil, the peripheral boundary of the test soil tank was compacted to reduce the influence of the boundary effect. Ridges were built on the tilth layer with a height of 15 cm, spacing of 65 cm, and soil bulk density of  $1.20 \text{ g/cm}^3$ .

(2) On the day before the experiment, the test soil tank was covered with gauze, and pre-rainfall was conducted at a rainfall intensity of 30 mm/h until runoff yield on the slope surface, which ensured the consistency of soil conditions in the early stage of the experiment. After pre-rainfall, the test soil tank was covered with plastic cloth to prevent the evaporation of soil moisture and slow down the formation of a crust. The rainfall for the experiment began after a resting period of 12 h.

(3) After the start of the formal rainfall experiment, the runoff and soil loss on the slope were carefully observed. When runoff occurred, the first sample was collected at

the outlet of runoff collector, followed by sample-collection every 3 min. If the contour ridge tillage becomes damaged because of runoff, samples should be taken every 1 min thereafter. After rainfall, the supernatant of the runoff sample was removed, and placed in an oven at a constant temperature of 105 °C. The sediment quality was determined after drying.

### ***Calculation of P factor and analysis of main influencing factors***

#### *P factor calculation*

The equation form of the USLE (Wischmeier and Smith, 1978; Renard et al., 1997) is:

$$A = RKLSCP \quad (\text{Eq.1})$$

Soil loss modulus  $A$  ( $\text{t}\cdot\text{hm}^{-2}$ ) is the soil loss at a given period.  $R$  is the rainfall erosivity factor ( $\text{MJ}\cdot\text{mm}\cdot\text{hm}^{-2}\cdot\text{h}^{-1}$ ) for any given period and is obtained by summing for each rainstorm, the product of total storm energy ( $E$ ) and the maximum 30-min intensity ( $I_{30}$ ).  $K$  is the soil erodibility factor ( $\text{t}\cdot\text{h}\cdot\text{MJ}^{-1}\cdot\text{mm}^{-1}$ ), which is defined as the rate of soil loss per unit of  $R$  as measured on a unit plot.  $L$  and  $S$  (dimensionless) are the slope and slope length factors respectively, and account for the effect of the topography on soil erosion.  $C$  is the coverage-management factor, which is defined as the ratio of soil loss from land with a specific vegetation to the corresponding soil loss from continuous fallow.  $P$  is the support practice factor (Eq. 1), which is defined as the ratio of soil loss with a specific support practice to the corresponding loss with up-and-down slope culture.

In Equations 2 and 3, the  $S$  factor can be calculated according to the slope  $\theta$  (°):

$$S = 10.8\sin\theta + 0.03, \theta < 5^\circ \quad (\text{Eq.2})$$

$$S = 16.8\sin\theta - 0.5, \theta = 5^\circ \quad (\text{Eq.3})$$

In calculating the  $P$  factor, the amount of soil loss caused by up-and-down slope culture should be determined; this refers to the amount of soil loss caused by longitudinal ridge tillage. Both LWR and LNR are longitudinal ridge tillage practices, with differences only in the ridge and furrow sizes. To obtain unified contrast objects in calculating the  $P$  factor, the tillage practice with larger overall soil loss in LWR and LNR should be considered as the contrast objects. The other four tillage practices can be considered as soil and water conservation effects. The  $P$  factor value in the single rainfall event was determined by the ratio of soil loss amounts observed in the artificial simulated rainfall experiments.

#### *Main influencing factors affecting P factor*

We analysed the main factors that could influence variation in the  $P$  factor, including rainfall, slope, and hydraulic characteristics, to obtain the equation for calculating the  $P$  factor.

The effects of rainfall and surface slope are characterised by  $R$  and  $S$ , respectively. The hydraulic characteristics of surface runoff are reflected mainly by roughness  $n$  and the Froude number  $Fr$  (Römken et al., 2002; Cremers et al., 2010; Omidvar et al., 2019):

$$n = R_h^{2/3} \cdot J^{1/2} \cdot V_{OV}^{-1} \quad (\text{Eq.4})$$

$$Fr = V_{OV}^{-1} \cdot (gR_h)^{-0.5} \quad (\text{Eq.5})$$

where  $n$  is a parameter comprehensively reflecting the influence of the roughness of the ridge furrow surface on water flow (Eq. 4);  $Fr$  is used to judge the state of water flow (Eq. 5);  $R_h$  is the hydraulic radius (m), which is the ratio of the cross-sectional area of the flow and the wetted perimeter, and the wetted perimeter refers to the perimeter of the runoff in contact with the ridge furrow profile;  $J$  is the hydraulic slope (m/m), i.e., the soil tank slope;  $g$  is the Gravitational acceleration;  $V_{OV}$  is the flow velocity (m/s) of runoff in the ridge furrow, and is obtained by dividing the runoff discharge in the ridge furrow by the cross-sectional flow area. In this study, the discharge of each ridge furrow was considered equal under the condition of longitudinal ridge tillage, and the  $V_{OV}$  was calculated based on the outlet runoff volume of the soil tank (Eq. 6).

$$V_{OV} = Q_r \cdot (Nr \cdot R_r)^{-1} \quad (\text{Eq.6})$$

where  $Q_r$  is the runoff volume (m<sup>3</sup>) measured by the flowmeter at the outlet of the soil tank,  $Nr$  is the number of furrows in the soil tank, and  $R_r$  is the cross-sectional flow area in the furrows.

#### *Analysis of suitable conditions for the application of tillage practices*

We suggested appropriate conditions for the implementation of the tillage practices, considering soil loss reduction by these various tillage practices under the combined conditions of different rainfall erosivities and slopes. With regard to contour ridge tillage, if the ridge is penetrated by runoff, the contour ridge is considered damaged. In such a case, concentrated surface runoff could be formed in a short time, resulting in a significant increase in the soil loss amount. The threshold of hydrological conditions for contour ridge failure were analysed in this study.

## **Results**

### ***Runoff and soil loss under different tillage practices***

The runoff depth and soil loss modulus of the five tillage practices, namely NT, LWR, LNR, CWR, and CNR under extreme rainfall conditions are shown in *Figure 3*. Generally, the order of the runoff depth ( $D$ ) of the various tillage practices was LNR > LWR > NT > CNR > CWR. The order of the soil loss modulus ( $A$ ) was CNR > LNR > CWR > LWR > NT. Under extreme rainfall conditions, the soil loss amount of the contour ridge tillage was higher than that of the longitudinal ridge tillage, which was the opposite of the observation data of the runoff plot in a short time series (Xin et al., 2019). Therefore, to analyse the effect of water and soil loss reduction by soil conservation tillage practices, it was necessary to consider extreme rainfall conditions.

If the product ( $RS$ ) of rainfall erosivity  $R$  and slope factor  $S$  is used to characterise the interaction of rainfall and slope on the soil loss process, the runoff depth ( $D$ ) of various tillage practices has a significant linear function relationship with  $RS$  (*Fig. 4a*). The soil loss modulus ( $A$ ) of the tillage practice has a significant exponential increasing



relationship with  $RS$  (Fig. 4b). Generally, the increasing rate of  $D$  with the increase in  $RS$  is relatively stable, and the increasing rate of the contour ridge tillage is slightly higher than is that of the longitudinal ridge tillage. However, when  $RS$  was  $\geq 15 \text{ MJ}\cdot\text{mm}/(\text{hm}^2\cdot\text{h})$ , the increasing rate of  $A$  of all tillage practices increased with  $RS$ . Among these, the increasing rate of the soil loss modulus in CNR was the largest, even a little higher than it was in the LNR. During continuous heavy rainfall, a large amount of runoff collected gradually in the furrows in contour ridges. If the contour ridge was damaged under the effects of continuous runoff scouring, a large amount of runoff can be formed in a short time to scour the surface, resulting in substantial soil loss. Compared with other tillage practices, with NT it was not easy to form a concentrated confluence path on the surface that weakens the scouring and erosion capacity of per unit runoff.

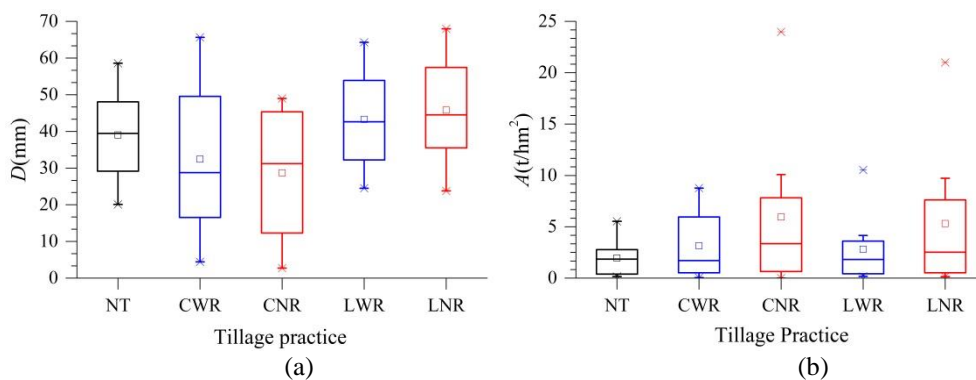


**Figure 3.** Relationship between runoff depth (a) and soil loss modulus (b) of various tillage practices

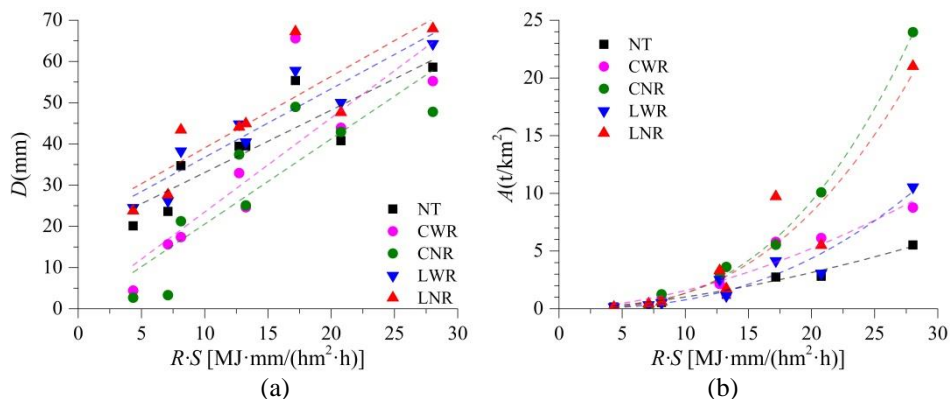


**Figure 4.** Relationship of  $RS$  with runoff depth (a) and soil loss modulus (b)

### ***P* factor under different tillage practices**

Under extreme rainfall conditions, the soil loss modulus of LWR varied from 0.17 to 10.54  $\text{t}\cdot\text{hm}^2$ , with an average of 2.80  $\text{t}\cdot\text{hm}^2$ . The soil loss modulus of LNR varied from 0.14 to 21.01  $\text{t}\cdot\text{hm}^2$ , with an average of 5.31  $\text{t}\cdot\text{hm}^2$ , i.e., the latter was generally higher. Therefore, LNR was considered the contrast object when calculating the  $P$  factor, LWR, CWR, CNR and NT could all be regarded as soil conservation tillage practices. See

Figure 5 for calculated P factor values. Among these, the P factor of LWR varied from 0.426 to 1.223, with an average of 0.712; the P factor of NT varied from 0.263 to 1.094, with an average of 0.634; the P factor of CWR varied from 0.302 to 1.375, with an average of 0.706; and the P factor of CNR varied from 0.051 to 2.090, with an average of 1.097. Clearly, the P factor value of NT was the lowest and, generally, there was little difference between LWR and CWR, whereas the P factor value of CNR was significantly higher than those of other tillage practices.

Regarding CWR, if the contour ridge was not damaged during the runoff yield, the average P factor value was 0.384. In case of damage, the average P factor value was 0.813. As regards CNR, the average P factor value was only 0.067 if the contour ridge was not damaged during the runoff yield. In case of damage, the average P factor value was 1.440. When other conditions were the same, if the contour ridge was damaged, the soil loss amount of the slope surface was close to or higher than that of longitudinal ridge tillage. Further, a concentrated runoff path could be formed in a short time, leading to a large amount of concentrated runoff scouring and resulting in more substantial soil loss.

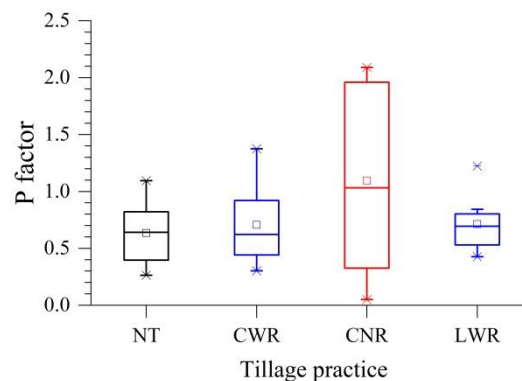


Figure 5. P factor values under various tillage practices

### Main factors affecting the P factor

#### Combined influence of rainfall intensity and slope

For NT and LWR, there was a significant logarithmic decreasing relationship between the P factor value of a single runoff event and  $RS$  (Fig. 6):

$$NT: P_{NT} = -0.392 \ln(RS) + 1.607, (r^2 = 0.69, p < 0.05) \quad (\text{Eq.7})$$

$$LWR: P_{LWR} = -0.364 \ln(RS) + 1.616, (r^2 = 0.80, p < 0.01) \quad (\text{Eq.8})$$

Along with the increase in rain intensity and slope, the relative soil loss reduction effect of NT and LWR was more significant. For LNR, the average height difference between the adjacent lowest point of the ridge furrow and the highest point of the contour ridge was 15 cm, and the average horizontal distance between them was 30 cm, with the ratio being 0.50. For LWR, the average height difference of the highest points of the two was reduced to 10 cm, and the average horizontal distance was expanded to 55 cm, with the ratio being 0.18, i.e., significantly lower than was that of the former. The amount of soil loss in the process of extreme rainfall was relatively low on the

surface of sloping farmland with micro-topographic relief. Regarding farmlands with a long, gentle slope, the amount of soil loss could be reduced in the process of runoff scouring by appropriately reducing the degree of micro-topographic relief.

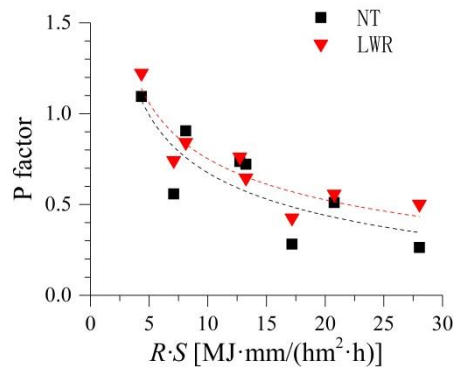


**Figure 6.** Relationship of P factor value with rainfall erosivity (R) and slope factor (S) under extreme rainfall conditions

#### Hydraulic characteristics of longitudinal ridge tillage

Roughness ( $n$ ) and Froude number ( $Fr$ ) are important parameters that affect the soil loss process of the slope surface under longitudinal ridge tillage. For LWR,  $n$  varied from 0.124 to 0.227, with an average of 0.191, and for LNR,  $n$  varied from 0.061 to 0.144, with an average of 0.100. Research has suggested that  $n$  of bare ridge tillage farmland is 0.06 to 0.12, and an average value of 0.09 is adopted usually when no actual measurement is conducted (Neitsch et al., 2002). The variation range of  $n$  under LNR was slightly higher than the suggested range, whereas the  $n$  value under LWR was generally higher than this range. In our study, the Manning roughness coefficient  $n$  reflected the blocking effect of the roughness of furrows on water flow. The typical black soil areas in Northeast China have a gentle slope, and the depth of runoff in furrows is shallow, mostly less than 2 cm, which leads to an increase in  $n$ . Compared with LNR, LWR had greater width at the bottom of furrows and shallower depth of water flow; therefore, it had a greater blocking effect on runoff from the slope surface. This effect could reduce the flow velocity on the slope surface, thereby reducing the soil loss and scouring from the runoff.

As regards the flow pattern in the furrows, the  $Fr$  under LWR and LNR varied from 0.147 to 0.619, with an average of 0.297. The  $Fr$  values were all greater than 0.10, which showed that the flow pattern in the furrows was slow. Generally, the  $Fr$  value under LNR was slightly higher. There is a significant quadratic relationship in the  $n$  and  $Fr$  values of LWR with  $RS$  (Fig. 7):

$$n = -0.0004 (RS)^2 + 0.0154RS + 0.0776 \quad (\text{Eq.9})$$

$$Fr = 0.0005(RS)^2 - 0.0173RS + 0.322 \quad (\text{Eq.10})$$

With an increase in  $RS$ , the  $n$  value of furrows under LWR gradually increased, but the growth rate of the  $n$  value decreased significantly from  $RS \geq 15 \text{ MJ} \cdot \text{mm}/(\text{hm}^2 \cdot \text{h})$  (Fig. 7a). This indicated that with the increase in runoff, the blocking effect of the

surface on the slope runoff became limited gradually, leading to the soil loss modulus increasing significantly with an increase in  $RS$  (Fig. 4b) and the decline rate of the P factor value gradually slowing down (Fig. 6). There was no significant correlation of the  $n$  and  $Fr$  values of furrows under LNR with  $RS$  (Fig. 7b).

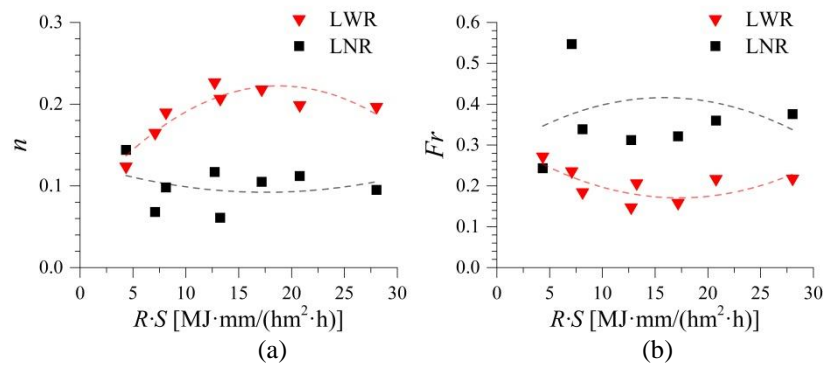


Figure 7. Relationship of  $RS$  with roughness (a) and Froude number (b)

### Suitable conditions for application of main tillage practices

Figure 8 shows the changes in soil loss rate with time under different experimental rainfall intensities. With a rainfall intensity of 30 mm/h, the soil loss rate under CNR was significantly lower than under NT or LWR. Although the soil loss rate under CWR increased significantly after 45 min, and was between that of NT and LWR (Fig. 8a), the average soil loss rate during the runoff yield process was still lower than under NT or LWR. With a rainfall intensity of 50 mm/h, the soil loss rates under CWR and CNR rapidly increased at 30 and 42 min, respectively, because the contour ridges had been damaged during the runoff yield; however, the average soil loss rates of the entire runoff yield process did not differ much from those under NT and LWR. With rain intensities of 75 and 100 mm/h, the time points of sudden increase in the soil loss rate under CWR and CNR advanced further, which were 21 and 33 min under 75 mm/h, and 19 and 33 min under 100 mm/h, respectively. The average soil loss rates under both tillage practices were significantly higher than those under NT and LWR. Compared with CWR, the soil loss rate under CNR increased faster after breaking the ridges. With 100 mm/h as an example, the soil loss rate under CNR increased by 173.0 times and that of CWR by 12.5 times within 6 min after breaking the ridge. The soil loss rates under NT and LWR showed little difference under conditions of 50 and 75 mm/h, and the soil loss rate under NT was lower than under LWR with conditions of 30 and 100 mm/h.

With extreme rainfall, soil loss caused by contour ridge failure is a significant source of soil loss and sediment yield on the slope surface under contour ridge tillage. Considering the test slope as a whole, the soil loss modulus  $Ar_w$  and  $Ar_n$  corresponding to contour ridge failure under CWR and CNR increased significantly linearly with  $RS$  (Fig. 9):

$$\text{CWR: } Ar_w = 1.65RS - 15.85, (R^2 = 0.73, p < 0.1) \quad (\text{Eq.11})$$

$$\text{CNR: } Ar_n = 5.09RS - 46.74, (R^2 = 0.96, p < 0.01) \quad (\text{Eq.12})$$

Although the slopes and intercepts of the above two linear equations were quite different, when contour ridge failure under CWR and CNR started to occur, the  $RS$  values were 9.61 and 9.18 MJ·mm/(hm<sup>2</sup>·h), respectively, i.e., considerably close to each other. These values could be used as the threshold of hydrological conditions for contour ridge failure.

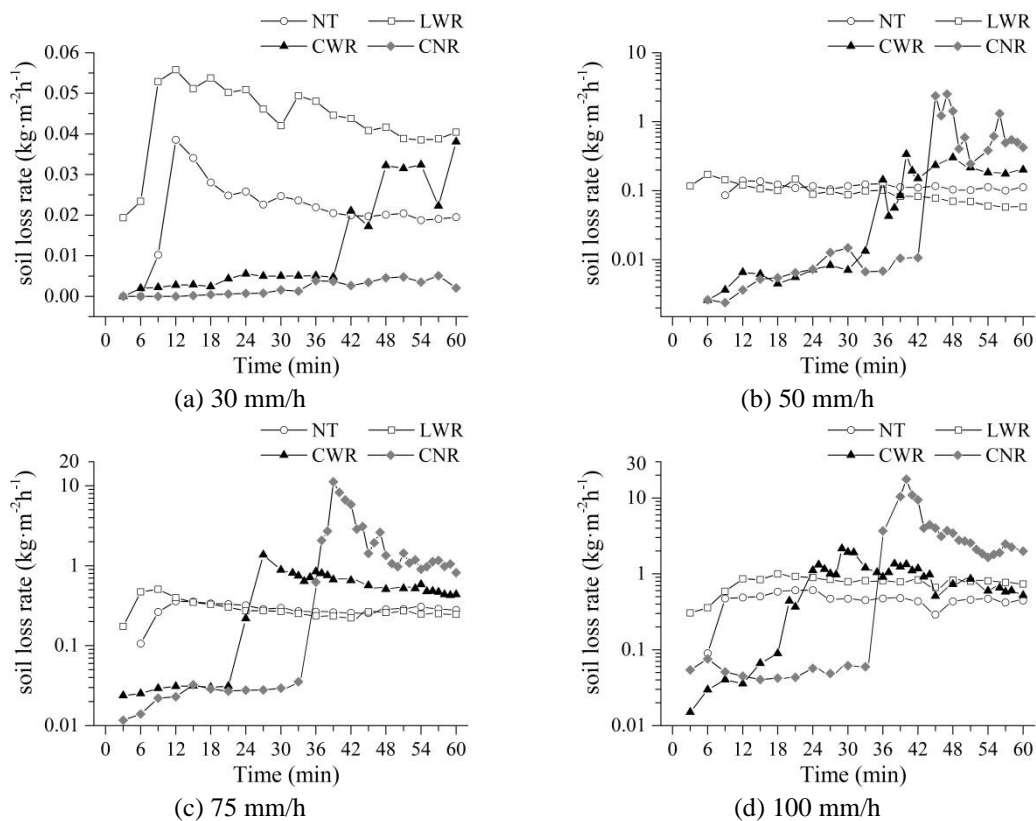


**Figure 8.** Changes in soil loss rate under various tillage practices under different rainfall intensities. Note: the average soil loss rate is the average value of soil loss rates under 3° and 5° under this tillage practice

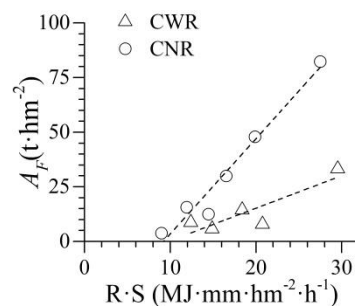


**Figure 9.** Relationship of soil loss modulus for contour ridge failure with rainfall erosivity and slope factor

According to the above analysis, when  $RS$  was < 9.18 MJ·mm/(hm<sup>2</sup>·h), contour ridge tillage was the optimal tillage practice to reduce soil loss. In a unit area, the impoundment

runoff of furrows under CNR was 2.08 times that of CWR, i.e., the effect of reducing water and sediment was more significant. When  $RS$  was  $\geq 9.18 \text{ MJ}\cdot\text{mm}/(\text{hm}^2\cdot\text{h})$  and the maximum rainfall intensity was  $< 75 \text{ mm/h}$ , there was no significant difference between CWR and NT in respect of the soil loss reduction effect. When the maximum rainfall intensity was  $> 75 \text{ mm/h}$ , NT had the optimal effect in reducing soil loss.

## Discussion

### *Comparison with annual average field observation values*

When the P factor value of this study was compared with the multi-year average P factor values observed in the runoff plots (Table 2), the former was substantially higher. The rainfall intensity of the artificial rainfall experiment was primarily designed based on the highest local 1 h rainfall intensity over 5–100 years. The observation of soil loss in this area began relatively late, and the continuous observation data of many field runoff plots cover no more than 5 years; consequently, the soil loss under extreme rainfall is not reflected fully. However, the soil loss caused by extreme rainfall accounted for a significant proportion of the total soil loss, and this fact should not be ignored. In the extreme rainfall events, soil loss of the LWR and LNR systems were both severe, and the P value increased. For most of the erosion event in the field runoff plot, the soil loss rates were relatively low without ridge failure, and the P factors were relatively low. While in the extreme rainfall events, after the ridge failure, the increasing trends for soil loss rates were significant, especially for higher rainfall intensities, and the P factors increased significantly. Accordingly, the amount of soil loss for CWR and CNR systems could be underestimated if the annual average P observed from the runoff plot was used in the calculations.

**Table 2.** Comparison between P factor value of this study and observation value of field runoff plot

Tillage practice	Observation time	Observation site	Slope (°)	Average P factor	Literature source
LWR	1 year	Keshan	5	0.33	Wang et al., 2019
	Extreme rainfall	Indoor (artificial rainfall)	3	0.81	This study
	Extreme rainfall	Indoor (artificial rainfall)	5	0.61	This study
CWR	6 years	Jiusan	5	0.08	Xin et al., 2019
	3 years	Binxian	6	0.12	Xin et al., 2019
	3 years	Zhalantun	7	0.05	Xin et al., 2019
	Extreme rainfall	Indoor (artificial rainfall)	3	0.73	This study
	Extreme rainfall	Indoor (artificial rainfall)	5	0.68	This study
CNR	3 years	Meihekou	7	0.39	Xin et al., 2019
	3 years	Fuxin	12	0.71	Xin et al., 2019
	Extreme rainfall	Indoor (artificial rainfall)	3	0.91	This study
	Extreme rainfall	Indoor (artificial rainfall)	5	1.29	This study

### *Differences in soil loss forms*

Indoor artificial rainfall observation showed that for NT, LWR, and LNR, the main forms of soil loss were sheet and inter-rill erosion, and no ephemeral gully erosion

occurred under any rainfall intensity. For CWR and CNR, if no contour ridge failure occurred, the soil loss form was mainly sheet and inter-rill erosion, with ephemeral gully erosion being rare. However, if contour ridge failure occurred, it led to the occurrence and aggravation of ephemeral gully erosion. After extreme rainfall, the width at contour ridge failure sites under CWR varied from 9 to 68 cm, with an average of 30.6 cm, and the maximum width at 92.3% of contour ridge failure sites exceeded 20 cm. The width at contour ridge failure sites under CNR varied from 7 to 138 cm, with an average of 33.1 cm, and the maximum width at 86.0% of contour ridge failure sites exceeded 20 cm. When the width of a rill on the slope surface exceeded 20 cm, it could easily develop into ephemeral gully erosion (Zhao et al., 2012). Therefore, generally, if contour ridge failure occurred because of rainfall runoff, it could easily induce ephemeral gully erosion.

With an increase in slope surface runoff, the width and volume of contour ridge failure soil loss enlarged correspondingly, resulting in the gradual occurrence and aggravation of ephemeral gully erosion (Douglas-Mankin et al., 2020). Using a single contour ridge as the analysis object, runoff is an important factor in the degree of contour ridge failure. There was a significant exponential increasing relationship between the failure volume  $V_F$  of a single contour ridge and the runoff  $Q$  in the corresponding catchment area of this contour ridge (Fig. 10a). With an increase in  $Q$ , the rate of increase of contour ridge failure in  $5^\circ$  narrow ridges was the fastest, the increase rate in contour ridge failure in  $3^\circ$  narrow ridges was the slowest, and the increase rate of contour ridge failure in wide ridges was between the two.

As shown in Figure 10b, there is a significant exponential increasing relationship between failure width  $W_F$  and  $Q$  of a single contour ridge in contour ridge tillage. Specifically (Eqs.13–15):

$$5^\circ \text{ CNR: } WF5 = 8.89\exp(2.42Q), (R^2 = 0.81, p < 0.01) \quad (\text{Eq.13})$$

$$3^\circ \text{ CNR: } WF3 = 11.96\exp(1.42Q), (R^2 = 0.44, p < 0.01) \quad (\text{Eq.14})$$

$$\text{CWR: } WFW = 15.71\exp(0.99Q), (R^2 = 0.59, p < 0.01) \quad (\text{Eq.15})$$

If  $W_F = 20$  cm is considered the critical value for the beginning of ephemeral gully erosion on the slope surface, and this value is substituted into Equations 13–15, it can be inferred that the threshold values of runoff in the upstream catchment for the contour ridge failure are 0.335, 0.362, and 0.244  $\text{m}^3$ , for substantial contour ridge failure in the  $5^\circ$  narrow ridge,  $3^\circ$  narrow ridge, and the wide ridge, respectively. The typical black soil areas in Northeast China have a gentle topography, with slopes mostly  $<5^\circ$  and a surface slope length mostly between 300 and 1500 m. The catchment area in the upper reaches of the farmland plot is large, and a large amount of surface runoff can be collected during the rainstorm process, which scours and damages the contour ridges and forms an ephemeral gully erosion path. The catchment area of a single plot could be reduced significantly by building a reasonable drainage or runoff diversion path, thereby realising the purposes of arranging water flow and reducing soil loss.

### ***Sediment deposition on slope surface under contour ridge tillage***

With regard to a slope surface with ephemeral gully erosion, the soil loss modulus  $A_F$  corresponding to the contour ridge failure during extreme rainfall was compared with



the slope soil loss modulus  $A$ . If  $A_F$  is considered the independent variable and  $A$  the dependent variable, the slope of the zero-crossing linear equation fitted by the two was only 0.267 (Fig. 11), which showed that an average of at least approximately 73% of the soil loss sediment was deposited in the slope surface confluence. The deposition sites were mainly the furrows. When contour ridge failure occurred, if the contour ridge located at its downstream was not damaged immediately, the soil loss sediment generated by the contour ridge failure could be easily deposited in the gullies. In some furrows, the deposited sediment blocked the horizontal movement of water in the furrow, forming a significant ephemeral gully erosion path (Fig. 12).

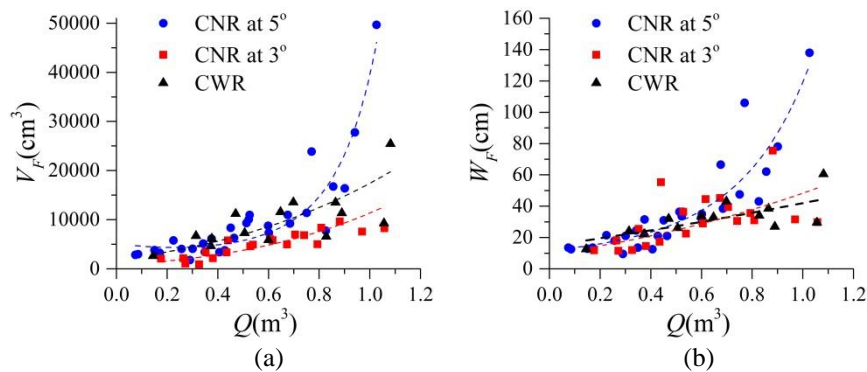


**Figure 10.** Relationship of failure volume (a) and failure width (b) of a single contour ridge with runoff in its upstream catchment

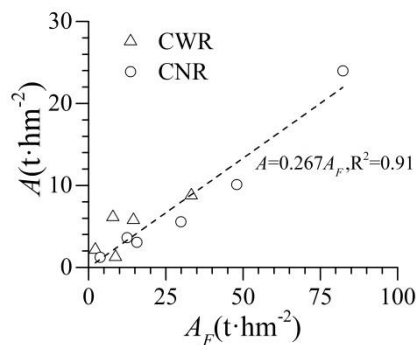


**Figure 11.** Relationship between slope soil loss modulus and sediment yield modulus in ephemeral gully erosion process

In their study, Gao et al. (2016) selected a small watershed with an area of 2.1 km<sup>2</sup>, with the proportion of farmland amounting to 95% in the typical black soil areas of Northeast China. Based on the observation data of soil loss and sediment yield, the average sediment delivery ratio in this watershed was calculated as 0.38. The analysis showed that most of the sediments from soil loss were deposited before entering the river channel, caused mainly by the topographic characteristics of gentle and long slopes. Because of the slow confluence speed, runoff could infiltrate easily and, coupled with the high summer temperature, evaporation was relatively strong. When surface runoff infiltrates and evaporates, the sediments carried by it would also deposit at the foot of a slope, meadow, and other places with gentle terrain or high surface resistance.



The accumulated water in the low-lying areas of the earth's surface contributes to soil loss materials being deposited easily. It should be recognised that furrows could serve as the location where a large amount of soil loss sediment is deposited (Fig. 12), which increases the complexity of sediment deposition in such areas.



**Figure 12.** Sediment deposition in furrows

## Conclusion

(1) In longitudinal ridge tillage practices, LNR, with a higher soil loss amount was considered the contrast object when calculating the P factor, and LWR, CWR, CNR, and NT were all regarded as soil conservation tillage practices. Under extreme rainfall conditions, the P factor of LWR varied from 0.426 to 1.223, with an average of 0.712; the P factor of NT varied from 0.263 to 1.094, with an average of 0.634; the P factor of CWR varied from 0.302 to 1.375, with an average of 0.706; and the P factor of CNR varied from 0.051 to 2.090, with an average of 1.097. The P factor value of NT was the lowest and, generally, there was not significant difference between LWR and CWR; the P factor value of CNR was significantly higher than those of other tillage practices.

(2) The P factor value is influenced by the combined action of rainfall erosivity( $R$ ) and the slope factor( $S$ ). For NT and LWR, there was a significant logarithmic decreasing relationship between the P factor value and  $RS$ . Under NT,  $P_{NT} = -0.392\text{Ln}(RS) + 1.607$ , and under LWR,  $P_{LW} = -0.364\text{Ln}(RS) + 1.616$ . On the surface of sloping farmland with relatively small topographic relief, the amount of soil loss in the process of extreme rainfall was relatively low. With an increase in  $RS$ , the  $n$  of furrows under LWR gradually increased; however, when  $RS$  was  $\geq 15 \text{ MJ}\cdot\text{mm}/(\text{hm}^2\cdot\text{h})$ , the growth rate of the  $n$  value decreased significantly. Further, the blocking effect of surface on the slope runoff gradually became limited, and the soil loss modulus increased significantly with the increase in  $RS$ .

(3) When  $RS$  was  $< 9.18 \text{ MJ}\cdot\text{mm}/(\text{hm}^2\cdot\text{h})$ , contour ridge tillage was the best tillage practice to reduce soil loss. In a unit area, the impoundment runoff of furrows under CNR was 2.08 times that of CWR, i.e., its effect of reducing water and sediment was more significant. When  $RS$  was  $\geq 9.18 \text{ MJ}\cdot\text{mm}/(\text{hm}^2\cdot\text{h})$  and the maximum rainfall intensity was  $\leq 75 \text{ mm/h}$ , there was no significant difference between CWR and NT in their soil loss reduction effect. If the maximum rainfall intensity was higher than  $75 \text{ mm/h}$ , NT showed the optimal effect in reducing soil loss.

(4) For CWR and CNR, if no contour ridge failure occurred, the soil loss form was primarily surface soil loss, with ephemeral gully erosion being rare. However, when contour ridge failure occurred, the damage failure and width increased exponentially with the runoff in the upstream catchment, which could easily lead to the development of ephemeral gully erosion. At least approximately 73% of the soil loss sediment was deposited in the slope confluence during the soil loss process, and the deposited sites were mainly furrows. Deposited sediment blocked the lateral communication of water flow between some furrows, forming a significant ephemeral gully erosion path.

Changing the microtopography and thus regulating the confluence path to shorten the slope length and construct a drainage path, is a potential conservation practice for reducing soil loss in contour ridge systems in the typical black soil region of Northeast China, especially in extreme rainfall events. Study for the potential conservation practices is needed in future.

**Acknowledgements.** This research was funded by the National Key Research and Development Program of China (Grant No.2018YFC0507002), and the IWHR Research & Development Support Program (Grant No. SE0145B132017).

## REFERENCES

- [1] Ahamed, T. R. N., Rao, K. G., Murthy, J. S. R. (2000): Fuzzy class membership approach to soil erosion modelling. – *Agricultural Systems* 63(2): 97-110.
- [2] Aksoy, H., Kavvas, M. L. (2005): A review of hillslope and watershed scale erosion and sediment transport models. – *Catena* 64(2-3): 247-271.
- [3] Arnell, N. W. (1999): Climate change and global water resources. – *Global Environmental Change* 9(99): S31-S49.
- [4] Bartholy, J., Pongrácz, R. (2007): Regional analysis of extreme temperature and precipitation indices for the Carpathian Basin from 1946 to 2001. – *Global & Planetary Change* 57(1-2): 83-95.
- [5] Batista, P. V. G., Davies, J., Silva, M. L. N., et al. (2019): On the evaluation of soil erosion models: are we doing enough? – *Earth-Science Reviews* 197: 102898.
- [6] Brazier, R. (2004): Quantifying soil erosion by water in the UK: a review of monitoring and modelling approaches. – *Progress in Physical Geography* 28(3): 340-365.
- [7] Chen, X., Cai, Q.G., Wang, X.Q. (2008): Suitability of soil and water conservation measures on sloping farmland in typical black soil region of Northeast China. – *Science of Soil Water Conservation* 6(5): 44-49 (in Chinese with English abstract).
- [8] Chen, D., Wei, W., Chen, L. (2017): Effects of terracing practices on water erosion control in china: a meta-analysis. – *Earth-Science Reviews* 173: 109-207.
- [9] Cremers, N. H. D. T., Dijk, P. M. V., Roo, A. P. J. D., Verzaandvoort, M. A. (2010): Spatial and temporal variability of soil surface roughness and the application in hydrological and soil erosion modelling. – *Hydrological Processes* 10(8): 1035-1047.
- [10] Cui, M., Cai, Q., Zhu, A., et al. (2007): Soil erosion along a long slope in the gentle hilly areas of black soil region in Northeast China. – *Journal of Geographical Science* 17(3): 375-383.
- [11] Di Stefano, C., Pampalone, V., Todisco, F., et al. (2019). Testing the Universal Soil Loss Equation-MB equation in plots in Central and South Italy. – *Hydrological Processes* 33(18): 2422-2433.
- [12] Douglas-Mankin, K. R., Roy, S. K., Sheshukov, A. Y., et al. (2020). A comprehensive review of ephemeral gully erosion models. – *Catena* 195: 104901.

- [13] Foster, G. R., Yoder, D. C., Weesies, G. A., Toy, T. J. (2001): The Design Philosophy Behind RUSLE2: Evolution of an Empirical Model. – In: Ascough, J. C. II, Flanagan, D. C. (eds.) *Soil Erosion Research for the 21st Century*, Proc. Int. Symp. (3-5 January 2001, Honolulu, HI, USA). ASAE, St. Joseph, MI, pp. 95-98.
- [14] Gassman, P. W., Reyes, M. R., Green, C. H., et al. (2007): The Soil and water assessment tool: historical development, applications, and future research directions. – *Trans. of the ASABE* 50(4): 1211-1250.
- [15] Ibearugbulem, O. H., Okoro, B. C., Osuagwu, J. C., Agunwamba, J. C. (2018): Development of empirical soil loss regression model (ESLRM). – *International Journal of Scientific and Engineering Research* 9(12): 2229-5518.
- [16] Khosravi, K., Safari, A., Habibnejad, R. M., Mahmoudi, N. (2012). Evaluation of soil erosion and sediment yield estimation various empirical model by observation values case study: Babolroud watershed, Mazandaran province. – *Environmental Erosion Research Journal* 1(4): 32-52.
- [17] Kinnell, P. I. A. (2010). Event soil loss, runoff and the Universal Soil Loss Equation family of models: a review. – *Journal of Hydrology* 385(1-4): 384-397.
- [18] Kinnell, P. I. A., Risse, L. M. (1998). USLE-M: empirical modeling rainfall erosion through runoff and sediment concentration. – *Soil Science Society of America Journal* 62(6): 1667-1672.
- [19] Lal, R. (2001): Soil degradation by erosion. – *Land Degrad. Dev.* 12(6): 519-539.
- [20] Lane, L., Renard, K., Foster, G., et al. (1992): Development and application of modern soil erosion prediction technology - the USDA experience. – *Soil Research* 30(6): 893-912.
- [21] Licznar, P., Nearing, M. A. (2003): Artificial neural networks of soil erosion and runoff prediction at the plot scale. – *Catena* 51(2): 89-114.
- [22] Liu, B. Y., Zhang, K. L., Xie, Y. (2002). An Empirical Soil Loss Equation. – *Process of 12th International Soil Conservation Organization Conference*. Tsinghua Press, Beijing, pp. 143-149.
- [23] Liu, B. Y., Yan, B. X., Shen, B., et al. (2008): Current status and comprehensive control strategies of soil erosion for cultivated land in the Northeastern black soil area of China. – *Science of Soil and Water Conservation* 6(1): 1-8.
- [24] Lobo, G. P., Bonilla, C. A. (2019): Predicting soil loss and sediment characteristics at the plot and field scales: model description and first verifications. – *Catena* 172: 113-124.
- [25] Lu, J., Zheng, F.L., Li, G.F., Bian, F., An, J. (2016): The effects of raindrop impact and runoff detachment on hillslope soil erosion and soil aggregate loss in the Mollisol region of Northeast China. – *Soil Tillage Res.* 161: 79-85.
- [26] Mausbach, M. J., Dedrick, A. R. (2004): The length we go-measuring environmental benefits of conservation practices. – *Journal of Soil and Water Conservation* 59(5): 96-103.
- [27] Meng, L.Q., Li, Y. (2009): The mechanism of gully development on sloping farmland in black soil area, Northeast China. – *Journal of Soil and Water Conservation* 23(1): 7-11 (in Chinese with English abstract).
- [28] Nearing, M. A., Foster, G. R., Lane, L. J., Finkner, S. C. (1989): A process-based soil erosion model for usda-water erosion prediction project technology. – *Transactions of the ASAE* 32(5): 1587-1593.
- [29] Neitsch, S. L., Arnold, J. J., Kiniry, J. R. (2002): *Soil and Water Assessment Tool: Theoretical Documentation*, version 2000. – Texas Water Resources Institute, Texas, pp. 235-238.
- [30] Nouwakpo, S. K., Weltz, M. A., Awadis, A., Green, C. H., Al-Hamdan, O. Z. (2018): Process-based modeling of infiltration, soil loss, and dissolved solids on saline and sodic soils. – *Transactions of the ASABE* 61(3): 1033-1048.
- [31] Ohmura, A., Wild, M. (2002): Is the hydrological cycle accelerating? – *Science* 298(5597): 1345-1346.

- [32] Omidvar, E., Hajizadeh, Z., Ghasemieh, H. (2019). Sediment yield, runoff and hydraulic characteristics in straw and rock fragment covers. – *Soil and Tillage Research* 194: 104324.
- [33] Renard, K. G., Forster, G. R., Weesies, G. A., et al. (1997): Predicting Soil Erosion by Water: A Guide to Conservation Planning with the Revised Universal Soil Loss Equation (RUSLE). – USDA Agric. Handb. No. 703, U.S. Gov. Print. Office, Washington, DC.
- [34] Römken, M. J. M., Helming, K., Prasad, S. N. (2002): Soil erosion under different rainfall intensities, surface roughness, and soil water regimes. – *Catena* 46(2-3): 103-123.
- [35] Shen, H. O., Wang, D. L., Wen, L. L., Zhao, W. T., Zhang, Y. (2020): Soil erosion and typical soil and water conservation measures on hillslopes in the Chinese Mollisol region. – *Eurasian Soil Science* 53(10): 1509-1519.
- [36] Shoemaker, L., Dai, T., Koenig, J. (2005): TMDL Model Evaluation and Research Needs. – Remediation and Pollution Control Division, National Risk Management Research Laboratory, Cincinnati.
- [37] Singh, P., Kumar, N. (1997): Impact assessment of climate change on the hydrological response of a snow and glacier melt runoff dominated Himalayan river. – *Journal of Hydrology* 193(1-4): 316-350.
- [38] Stocker, T. F., Qin, D., Plattner, G. K., Tignor, M., Allen, S. K., Boschung, J., et al. (2013): IPCC, 2013: climate change 2013: the physical science basis. Contribution of working group I to the fifth assessment report of the intergovernmental panel on climate change. – *Computational Geometry* 18(2): 95-123.
- [39] Tyner, J. S., Yoder, D. C., Chomicki, B. J., Tyagi, A. (2011): A review of construction site best management practices for erosion control. – *Transactions of the ASABE* 54(2): 441-450.
- [40] Van der Kinff, J. M., Jones, R. J. A., Montanarella, L. (2000): Soil erosion risk assessment in Europe. – European Commission, Directorate General JRC, Joint Research Centre, Space Application Institute, European Soil Bureau.
- [41] Wang, Z. Q., Liu, B. Y., Wang, X. Y., Gao, X. F., Liu, G. (2009): Erosion effect on the productivity of black soil in Northeast China. – *Science in China* 52(007): 1005-1021.
- [42] Wang, J., Xie, Y., Liu, G., et al. (2015): Soybean root development under water stress in eroded soils. – *Acta Agric. Scand.* 65(4): 374-382.
- [43] Wang, L., Shi, H. Q., Liu, G., Zheng, F. L., Qin, C., Zhang, X. C., Zhang, J. Q. (2019): Comparison of soil erosion between wide and narrow longitudinal ridge tillage in black soil region. – *Transactions of the Chinese Society of Agricultural Engineering* 35(19): 176-182 (in Chinese with English abstract).
- [44] Williams, J. R. (1975): Sediment-yield prediction with universal equation using runoff energy factor. – *Proceedings of the Sediment-Yield Workshop. Present and Prospective Technology for Predicting Sediment Yield and Sources.* USDA Sedimentation Lab, Oxford, MS, pp. 244-252.
- [45] Williams, J. R., Dyke, P. T., Jones, C. A. (1983): A new method for assessing the effect of erosion on productivity - the EPIC model. – *Journal of Soil and Water Conservation* 38: 381-383.
- [46] Wischmeier, W. H., Smith, D. D. (1958): Rainfall energy and its relationship to soil loss. – *Transactions of American Geophysical Union* 39(2): 285-291.
- [47] Wischmeier, W. H., Smith, D. D. (1965): Predicting Rainfall-Erosion Losses from Cropland East of the Rocky Mountains: Guide for Selection of Practices for Soil and Water Conservation. – *Agric. Handbook. No.282.* U.S. Dep. Agric., Washington, DC.
- [48] Wischmeier, W. H., Smith, D. D. (1978): Predicting Rainfall Erosion Losses: A Guide to Conservation Planning. – *Agric. Handbook. No.537.* U.S. Dep. Agric., Washington, DC.
- [49] Xin, Y., Liu, G., Xie, Y., Gao, Y., Liu, B. Y., Shen, B. (2019): Effects of soil conservation practices on soil losses from slope farmland in northeastern China using runoff plot data. – *Catena* 174: 417-424.

- [50] Xu, X. M., Zheng, F. L., Wilson, G. V., He, C., Lu, J., Bian, F. (2018): Comparison of runoff and soil loss in different tillage systems in the Mollisol region of Northeast China. – Soil and Tillage Research 177: 1-11.
- [51] Xu, X. M., Zheng, F. L., Qin, C., Han, Y. (2019): Dynamic monitoring of ephemeral gully development and its morphology quantification in loess hilly-gully region. – Transactions of the Chinese Society for Agricultural Machinery 50(4): 274-282 (in Chinese with English abstract).
- [52] Ye, D. X., Zhang, C. J., Zhou, Z.J. (2014). Climatological Atlas of Extreme Precipitation in China. – Meteorological Press, Beijing, pp. 119-123.
- [53] Yu, B. (1999): A comparison of the R-factor in the USLE and RUSLE. – Transactions of the ASAE 42(6): 1615-1620.
- [54] Zhang, B., He, H. B., Ding, X. L., Zhang, X. D., Zhang, X. P., Yang, X. M., Filley, T. R. (2012). Soil microbial community dynamics over a maize (*Zea mays* L.) growing season under conventional- and no-tillage practices in a rainfed agroecosystem. – Soil and Tillage Research 124: 153-160.
- [55] Zhao, Y. M., Liu, B. Y., Jiang, H. T. (2012). Distribution of tillage-induced direction and its effect on soil erosion in black soil area of Northeast China. – CNKI 19(5): 1-6 (in Chinese with English abstract).

## APPENDIX

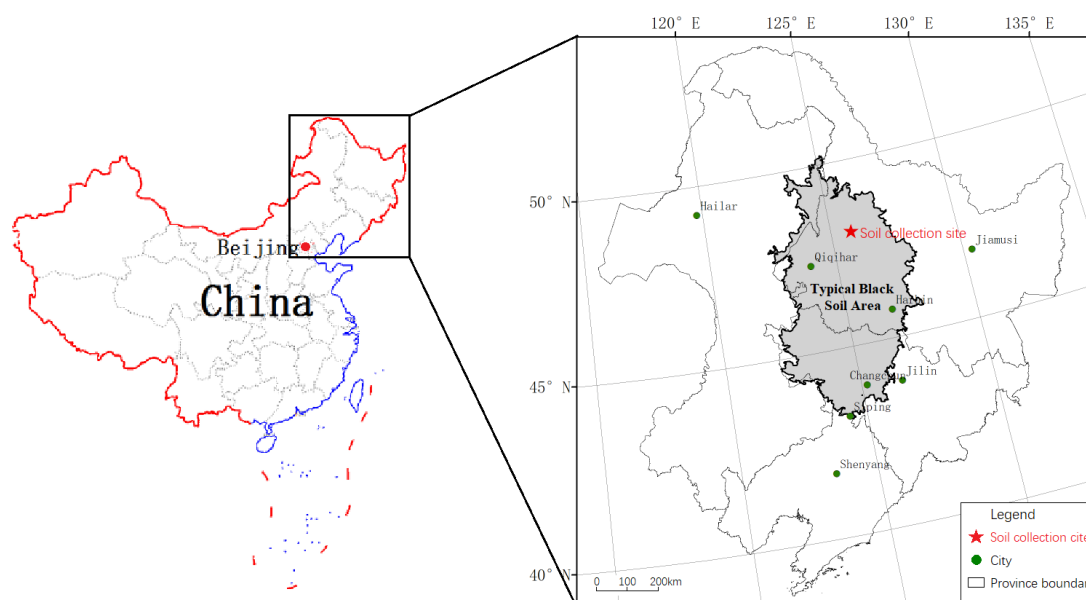


**Figure A1.** Location of the soil collection site